J. Am. Chem. Soc. **1991**, *113*, 4192-4198

Silver Trifluoride: Preparation, Crystal Structure, Some Properties, and Comparison with AuF_3[†]

Boris Žemva,[‡] Karel Lutar,[‡] Adolf Jesih,[‡] William J. Casteel, Jr.,[§] Angus P. Wilkinson,[⊥] David E. Cox,[∥] Robert B. Von Dreele,[∇] Horst Borrmann,[§] and Neil Bartlett*[,§]

Contribution from the Chemical Sciences Division, Lawrence Berkeley Laboratory, and Department of Chemistry, University of California, Berkeley, California 94720, Institute Jožef Stefan, University of Ljubljana, 61000 Ljubljana, Slovenia, Department of Chemical Crystallography, The University of Oxford, Oxford, England OX1 3PD, Department of Physics, Brookhaven National Laboratory, Upton, Long Island, New York, 11973, and Manuel Lujan, Jr., Neutron Scattering Center, Los Alamos National Laboratory, Los Alamos, New Mexico 87545.

Received November 30, 1990

Abstract: Red, diamagnetic AgF_3 is precipitated from anhydrous hydrogen fluoride (AHF) solutions of AgF_4^- salts by addition of fluoro acids (L) such as BF_3, PF_5, or AsF_5: $AgF_4^- + L \rightarrow AgF_3 + LF^-$. With additional AsF_5, silver(III) is reduced: $AgF_3 + AsF_5 \rightarrow AgFAsF_6 + {}^1/_2F_2$. Such reduction does not occur with BF_3, and the latter acid is therefore preferred for the preparation of stoichiometric AgF_3. AgF_3 is thermodynamically unstable and, in contact with AHF, at ~20 °C, loses F_2 in less than 19 h according to the equation $3AgF_3 \rightarrow Ag_3F_8 + {}^1/_2F_2$. The trifluoride is isostructural with AuF_3. To provide for meaningful comparisons, the structure of AuF_3 was redetermined. AgF_3 and AuF_3 were successfully refined in space group $P6_122\text{-}D_{62}$ (No. 178) by using the Rietveld method from time-of-flight neutron powder diffraction data from 100-mg samples contained in 2-mm capillary tubes. The 7762 observations for AgF_3 yielded $a = 5.0782$ (2) Å, $c = 15.4524$ (8) Å, and $V = 345.10$ (2) Å^3, the reliability parameters for the structure being $R_{wp} = 6.21$ and $R_p = 3.83\%$. From the 7646 observations for AuF_3, $a = 5.1508$ (1) Å, $c = 16.2637$ (7) Å, $V = 373.68$ (2) Å^3, and $R_{wp} = 11.21$ and $R_p = 7.58\%$. The silver or gold atom lies at the center of an elongated octahedron with two Ag–F(1) = 1.990 (3) Å, two Au–F(1) = 1.998 (2) Å, two Ag–F(2) = 1.863 (4) Å, and two Au–F(2) = 1.868 (3) Å, the approximately square, isodimensional AF_4 units being joined by symmetrical μ-fluoro bridges (two F(1) in cis relationship in the AF_4 unit) to form the 6_1 (or 6_5) helical chains where Ag–F(1)–Ag = 123.2 (2)° and Au–F(1)–Au = 119.3 (2)°. The ~5-Å^3 smaller formula unit volume of AgF_3 compared with AuF_3 and the shorter *z* axis interatomic distance (Ag–F = 2.540 (4), Au–F = 2.756 (8) Å) are in accord with the tighter binding of the Ag(III) d-orbital electrons evident in the strong oxidizing properties of Ag(III). Interaction of AgF^+ with AgF_4^- (1:1) in AHF yields maroon $Ag^{II}Ag^{III}F_5$. The latter interacts with AgF_3 to yield $Ag^{II}Ag^{III}{}_2F_8$, which is identical with the product of the decomposition of AgF_3 at 20 °C in AHF and with the material previously described[1,2] as AgF_3. The magnetic susceptibility for $Ag^{II}Ag^{III}{}_2F_8$ obeys the Curie–Weiss law (4–280 K) with $\theta = -4.2$ (5)° and $\mu_{eff} = 1.924$ (3) μ_B.

Diamagnetic salts of the AgF_4^- ion were first described by Hoppe[3] in 1957 and shown by him to be isomorphous with their AuF_4^- relatives. The Ag(III) salts were made by the fluorination of mixtures of binary nitrates or halides (e.g., $KAgF_4$ from fluorine on $KNO_3/AgNO_3$). The structural relationship of the alkali-metal tetrafluoroargentates(III) to the tetrafluoroaurates(III) was established by Hoppe and Homann,[4] and they found the interatomic distances in the square anions to be 1.90 Å for Ag–F and 2.00 Å for Au–F. They also noted that the formula unit volume of the fluoroargentate(III) was in each case smaller than that of the corresponding fluoroaurate(III). More recently, Lutar, Jesih, and Žemva used[5] krypton difluoride in anhydrous hydrogen fluoride (AHF) to prepare an AgF_4^- salt at room temperature, but related studies[6] failed to find evidence of oxidation beyond Ag(III) by this most powerful of oxidative fluorinators, despite the relative ease of oxidation by that reagent of AuF_4^- to AuF_6^-.

The much more demanding Ag(III) synthesis, entailed in making the binary fluoride, AgF_3, was first claimed by Bougon and Lance[1] in 1983. They described a red-brown, highly reactive solid, made by fluorination of the metal or its mono- or difluoride in AHF, by KrF_2 at room temperature. The reported X-ray powder diffraction data[1,2] showed that the red-brown solid was not structurally related to AuF_3.[7] Moreover, the solid, made in this way, proved to be weakly paramagnetic,[2] and this raised the possibility of some of the Ag(III) being in the triplet state. High-spin d^8 in Ag(III) had been described by Hoppe et al.[8] for the mixed-alkali-metal salt Cs_2KAgF_6, thus showing that low-spin d^8 is not decisively preferred for Ag(III) in a fluoroligated environment. More recently, AgF_3 was also claimed by Kiselev et al.[9] to be formed in the interaction of AgF_2 with O_2F_2 in ClF_5. The X-ray powder diffraction data for their material were indexed on the basis of a hexagonal unit cell with $a_0 = 8.989$ (5) and $c_0 = 9.815$ (5) Å, but not isomorphous with AuF_3. A crystal structure was not derived.

Recently, a general approach to polymeric binary fluoride synthesis has been discovered[10] in these laboratories in which the fluoride is liberated from its anion in AHF solution by a stronger fluoro acid. Even thermodynamically unstable binary fluorides can be made in this way. AgF_3 precipitates, as a bright-red solid, when AgF_4^- salts in AHF are treated with either AsF_5 or BF_3 (each represented by L): $AgF_4^- + L \rightarrow AgF_3 + LF^-$. It is isostructural with AuF_3 and is diamagnetic. This paper describes the preparation, structure, and some properties of this novel fluoride and demonstrates that the previously claimed AgF_3 is the mixed-valence compound $Ag^{II}Ag^{III}{}_2F_8$. A second mixed-valence compound, $Ag^{II}Ag^{III}F_5$, is also briefly described.

Results and Discussion

Silver trifluoride was precipitated from solutions of AgF_4^- salts in AHF, as a bright-red solid isomorphous with AuF_3, when AsF_5

[†] Dedicated to Professor Hans-Georg von Schnering on the occasion of his 60th birthday.

[§] University of California.

[‡] Institut Jožef Stefan.

[⊥] The University of Oxford.

[∥] Brookhaven National Laboratory.

[∇] Los Alamos National Laboratory.

(1) Bougon, R.; Lance, M. *C. R. Seances Acad. Sci., Ser. 2* **1983**, *297*, 117.

(2) Bougon, R.; Bai Huy, T.; Lance, M.; Abazli, H. *Inorg. Chem.* **1984**, *23*, 3667.

(3) Hoppe, R. *Z. Anorg. Allg. Chem.* **1957**, *292*, 28.

(4) Hoppe, R.; Homann, R. *Z. Anorg. Allg. Chem.* **1970**, *379*, 193.

(5) Lutar, K.; Jesih, A.; Žemva, B. *Rev. Chimie Miner.* **1986**, *23*, 565.

(6) Lutar, K.; Jesih, A.; Leban, I.; Žemva, B., Bartlett, N. *Inorg. Chem.* **1989**, *28*, 3467.

(7) Einstein, F. W. B.; Rao, P. R.; Trotter, J.; Bartlett, N. *J. Chem. Soc. A* **1967**, 478.

(8) Hoppe, R.; Homann, R. *Naturwissenschaften* **1966**, *53*, 501.

(9) Kiselev, Yu M.; Popov, A. I.; Timakov, A. A.; Bukharin, K. V.; Sukhoverkhov, V. F. *Zh. Neorg. Khim.* **1988**, *33*, 1252.

(10) Žemva, B.; Lutar, K.; Jesih, A.; Casteel, W. J. Jr.; Bartlett, N. *J. Chem. Soc., Chem. Commun.* **1989**, 346.

0002-7863/91/1513-4192$02.50/0

Table I. Selected Distances (Å) and Angles (deg) for AgF_3 and AuF_3

dist	Ag	Au	angle	Ag	Au
M–F(1) × 2	1.990 (3)	1.998 (2)	F(1)–M–F(1)	89.5 (2)	90.4 (2)
M–F(2) × 2	1.863 (4)	1.876 (3)	F(1)–M–F(2) × 2	90.6 (1)	89.6 (1)
M–F(2) × 2	2.540 (4)	2.761 (3)	F(2)–M–F(2)	176.6 (2)	177.5 (2)
			F(2)–M–F(2)	89.3 (3)	90.4 (2)
M–F(1)–M	123.2 (2)	119.4 (2)	M–F(2)–M	140.2 (2)	142.6 (2)

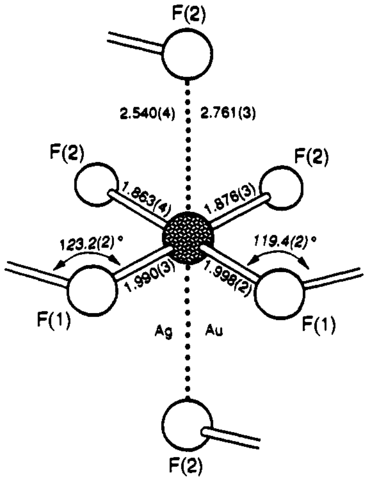

Figure 1. Interatomic distances (Å) for the elongated octahedral F ligand arrangement about the metal atom in AgF_3 and AuF_3 (estimated standard deviations in parentheses).

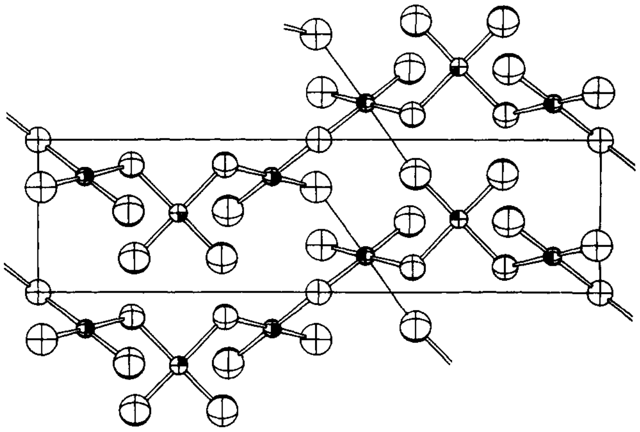

Figure 2. View down *a* showing unit cell contents and the F(2) interchain bridging in AgF_3 and AuF_3.

Table II. Comparison of Formula Unit Volumes (Å^3) of Ag(III) and Au(III) Compounds

A	XeF_5AF_4	KAF_4	AF_3	$AO_{3/2}$
Ag	159.4[a]	97.0[b]	57.5[c]	61.9[d]
Au	164.5[a]	102.1[b]	62.3[c]	64.7[e]

[a] Reference 6. [b] Reference 4. [c] Present work. [d] Reference 11. [e] Reference 12.

was added to those solutions. However, even when the mixture was well stirred, and the AsF_5 was added slowly, there was contamination of the AuF_3-like AgF_3 by a second phase, the X-ray diffraction pattern of which corresponded with that attributed to AgF_3 by Bougon et al.[1,2] This latter phase was not present when either PF_5 or BF_3 was substituted for AsF_5. Although PF_5 was able to precipitate AgF_3 from AgF_4^- in AHF, when an overpressure of the gas was maintained, the AgF_3 proved to be close enough in acidity to PF_5 that it redissolved when the overpressure of PF_5 was released. Boron trifluoride, however, proved to be a sufficiently superior acid to AgF_3 to bring about its complete precipitation with low BF_3 partial pressure:

$$AgF_4^- + BF_3 \rightarrow AgF_3 + BF_4^- \qquad (1)$$

The freshly precipitated bright red solid produced in this instance was diamagnetic, and its X-ray powder diffraction pattern was entirely accounted for by the AuF_3-like phase.

In its essentials, the structure of AgF_3 is the same as that of AuF_3.[7] The dimensions of the two fluorides are compared in Table I, and their structures are illustrated in Figures 1 and 2. The planar and approximately square AF_4 units (A = Ag or Au) that are joined by the symmetrical sharing of cis-related F(1) ligands to generate the helical chains of 6_1 or 6_5 symmetry, are almost isodimensional, the observed differences being barely significant. The bridging A–F–A angle of ~120° testifies to considerable covalency in the AF_4 unit bonding, in harmony with high electronegativity of the A(III) in the σ bonding. It is in the interaction of the helical chains with one another (see Figure 2) where the F(2) ligands of one chain approach approximately normal to the nearly square AF_4 unit of an adjacent chain that the greatest difference in the two structures appears. The elongation of the roughly octahedral arrangement is much greater for the AuF_6 group than for the AgF_6 one. This and the formula unit volume distinguish AgF_3 structurally from AuF_3. These features both point to the remaining valence electrons of Ag(III) being more tightly bound than in Au(III).

The formula unit volume of AgF_3 is approximately 5 Å^3 smaller than that of AuF_3. A similar contraction of Ag(III) relative to Au(III) occurs (see Table II) in the primitive unit cell volumes of the alkali-metal salts of AF_4^- (A = Ag or Au), in the salts[6] $XeF_5^+AF_4^-$, and in the oxides Ag_2O_3[11] and Au_2O_3.[12] This smaller effective size of the Ag(III) contrasts with the slightly larger effective size of silver, relative to gold, in the metals, in which the volume per atom[13] is 17.05 Å^3 for Ag and 16.97 Å^3 for Au. These observations can be accounted for (at least qualitatively) from consideration of relativistic effects. As Pitzer[14] and Pyykko and Desclaux[15] have separately pointed out, the relativistic effect (which is greatest for s electrons) stabilizes the s electrons of gold much more than the s electrons of silver. This contributes importantly to the smaller effective volume of metallic gold. But in each of the trifluorides of silver and gold, the s valence-shell electron has been largely lost to the fluorine ligands. The valence-shell electrons sterically available for bond formation that remain largely localized at the Ag(III) and Au(III) are $4d_{z^2}$ and $5d_{z^2}$, respectively. The greater *z*-axis interatomic distance (Figure 1) and larger effective volume in the AuF_3 case both point to the $d_z{}^2$ electron pair of Au(III) being less tightly bound (and hence bigger) than in the Ag(III) atom. This is consistent with the known relative atomic energy levels (see Pitzer,[14] Table IV). These features are also in harmony with the relative ease of oxidation[6] of Au(III) to Au(V). Tight binding of the Ag(III) d_{z^2} electron pair explains the failure[6] to prepare Ag(V) even with the most aggressive of oxidizers, KrF_2.

The weaker fluoro acid BF_3 produced higher purity AgF_3 than the stronger acid AsF_5, but it was necessary to remove AHF quickly from the AgF_3 because of its loss of fluorine in that solvent. AgF_3 stirred in AHF at 20 °C became dark red and slowly evolved fluorine gas. Within 19 h decomposition was complete, in accord with

$$3AgF_3 \rightarrow Ag_3F_8 + \tfrac{1}{2}F_2 \qquad (2)$$

---

(11) Standke, B.; Jansen, M. *Z. Anorg. Allg. Chem.* **1986**, *535*, 39.

(12) Jones, P. G.; Rumpel, H.; Schwarzmann, E.; Sheldrick, G. M. *Acta Crystallogr.* **1979**, *B35*, 1435.

(13) Wyckoff, R. W. G. *Crystal Structures*; Interscience Publishers: London, Sydney, 1963; Vol. 1.

(14) Pitzer, K. *Acc. Chem. Res.* **1979**, *12*, 271.

(15) Pyykko, P.; Desclaux, J. P. *Acc. Chem. Res.* **1979**, *12*, 276.

Table III. X-ray Powder Data for AgF_3[a] (Synchrotron Radiation, λ = 1.248 05 Å)

hkl	I/I_0	$1/d^2 \times 10^4$ obsd	calcd
100	31	518	518
101	21	560	560
102	19	685	685
103	100	895	895
104	6	1187	1188
006	5	1508	1509
110	10	1550	1553
105	10	1565	1565
111	5	1596	1595
112	12	1720	1720
113	2	1928	1930
106	10	2026	2026
200	5	2070	2070
114	1	2213	2223
202	19	2239	2238
203	3	2447	2448
107	4	2575	2571
115	25	2602	2600
204	16	2742	2741
116	12	3061	3062
108	3	3200	3200

[a] Hexagonal unit cell with (20 °C) a_0 = 5.0753 (3) Å, c_0 = 15.448 (1) Å, V = 344.62 (7) Å^3, Z = 6; space group $P6_122$-D_{62} or $P6_522$-D_{62}.

Table IV. X-ray Powder Data for Ag_3F_8 (Cu Kα, Ni Filter) at 20 °C

I/I_0	$1/d^2 \times 10^4$ (obsd)	I/I_0	$1/d^2 \times 10^4$ (obsd)
w	321	mw	2301
ms	482	vw	2410
mw	673	vw	2477
m	694	ms	2706
vvs	740	s(br)	2944
m	839	m	3269
ms	920	m	3457
mw	985	m	3524
vs	1087	ms	3682
mw	1142	m	3785
w	1322	s(br)	3830
m	1382	m	3924
w	1477	ms	4180
ms(br)	1603	ms	4340
m(br)	1706	m	4555
ms	1840	m	4686
s(br)	1940	m(br)	4891
vw	2038	vw	5296
m	2215	vw	5504

Thus, AgF_3 is thermodynamically unstable. When dry, however, AgF_3 has considerable kinetic stability and can be kept in quartz for several weeks, at 20 °C, and has withstood high-intensity X-radiation from a synchrotron source for several hours. Nevertheless, under the preparative conditions given by Bougon et al.[1,2] or by Kiselev et al.,[9] it is unlikely that AgF_3 was formed. Neither of the X-ray powder diffraction patterns, in those reports, corresponds with that of authentic AgF_3 given in Table III. There is, however, a close matching of the data of Bougon et al. with that given for Ag_3F_8 in Table IV, and the Kiselev et al. data also show a rough relationship to it.

The contamination of AgF_3, by Ag_3F_8, when precipitated by AsF_5, is a consequence of the reductive interaction of AgF_3 with AsF_5. Addition of excess AsF_5 over that required for the precipitation of AgF_3

$$AgF_4^- + AsF_5 \rightarrow AgF_3 + AsF_6^- \qquad (3)$$

brought about dissolution of the AgF_3, in AHF with reduction by the Ag(III) to Ag(II) according to

$$AgF_3 + AsF_5 \rightarrow AgFAsF_6 + \tfrac{1}{2}F_2 \qquad (4)$$

This must occur, to some extent, to the AgF_3 generated at the interface where AsF_5 meets AgF_4^- and where a local molar excess of the acid exists. A separate experiment, in which an $AgFAsF_6$ solution in AHF was mixed with 2 mol equiv of AgF_4^- and was then treated with BF_3, resulted in quantitative precipitation of the red-brown solid Ag_3F_8:

$$AgFAsF_6 + BF_3 + 2AgF_4^- \rightarrow Ag_3F_8 + AsF_6^- + BF_4^- \qquad (5)$$

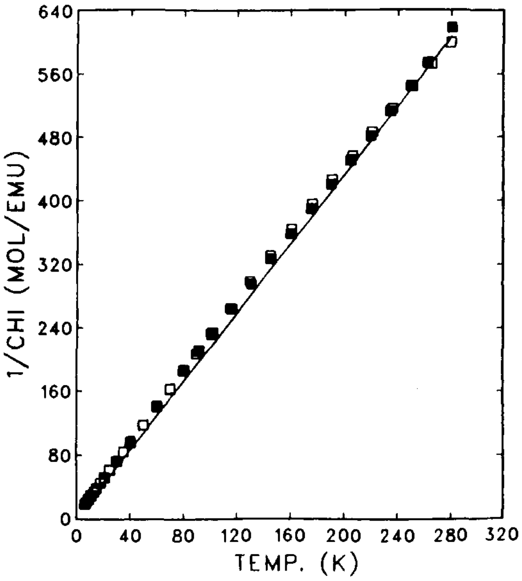

Figure 3. Curie–Weiss plot for Ag_3F_8: □, 5 kG; ■, 40 kG.

The X-ray powder diffraction pattern of this solid was identical with that of the Ag_3F_8 produced in the room-temperature decomposition of AgF_3 in AHF (eq 2). There was not detectable interaction of BF_3, in AHF with AgF_3, under the conditions used to precipitate the AgF_3 with that acid. Absence of reductive interaction of the BF_3 with the AgF_3 thus accounts for the high purity of AgF_3 obtained in that way.

It is probable that the superior fluoride ion affinity[16] of AsF_5 relative to BF_3 is responsible for the difference in reactivity of the two acids with AgF_3. The removal of F^- from Ag(III) would generate an exceptionally high electronegativity at silver in $[AgF_2]^+$. Electron capture, with fluorine release, is to be expected for Ag(III) in $[AgF_2]^+$ since even cationic Ag(II) possesses extraordinary oxidizing power[17] and is able to oxidize Xe to XeF_2 at 20 °C. The quantitative reduction of the AgF_3 by the action of the AsF_5, as expressed in eq 4, clearly signifies high oxidizing power for AgF_3, particularly in acidic AHF.

The anticipated high oxidizing power of AgF_3 is demonstrated by the interaction of the solid, in suspension in AHF, with Xe gas under ordinary temperatures and pressures:

$$2AgF_3 + Xe \rightarrow 2AgF_2 + XeF_2 \qquad (6)$$

Thus, AgF_3 is a more effective fluorine atom source than molecular F_2, with which Xe does not interact, in the absence of catalysts, under ordinary pressures and temperatures. It was, however, more surprising to find that even anionic Ag(III) will oxidize xenon spontaneously according to

$$2AgF_4^- + Xe \rightarrow 2AgF_2 + XeF_2 + 2F^- \qquad (7)$$

Clearly, Ag(III) in any fluoro ligand environment has a high enough electron affinity to be an effective source of fluorine atom ligands.

The formation of Ag_3F_8 by the interaction of 1 mol of Ag(II) with 2 mol of Ag(III) (as given in eq 5) confirmed that the material formed in the degradation of AgF_3 (eq 2) is a mixed-valence material, $Ag^{II}Ag^{III}_2F_8$. Given the diamagnetism of AgF_3, a low-spin d^8 configuration was expected for the two Ag(III) in the formula unit. These, it was anticipated, would separate the

---

(16) Mallouk, T. E.; Rosenthal, G. L.; Müller, G.; Brusasco, R.; Bartlett, N. *Inorg. Chem.* **1984**, *23*, 3167.

(17) Žemva, B.; Hagiwara, R.; Casteel, W. J., Jr.; Lutar, K.; Jesih, A.; Bartlett, N. *J. Am. Chem. Soc.* **1990**, *112*, 4846.

Table V. X-ray Powder Data for Ag_2F_5 (Cu Kα, Ni Filter) at 20 °C

I/I_0	$1/d^2 \times 10$ (obsd)	I/I_0	$1/d^2 \times 10$ (obsd)
vw	512	vw	2732
s(br)	670	ms	2882
vs	755	m	3049
s	896	vvw	3129
m	979	vw	3204
vvw	1068	vw	3294
s	1128	vvw	3366
ms	1245	ms(br)	3573
ms	1295	ms	3729
m	1445	vvw	3912
m	1575	vvw	4101
ms	1737	vvw	4217
vvw	1915	vvw	4319
vw	1956	vvw	4498
w	2109	vw	4790
s	2199	vvw	4982
vvw	2340	vvw	5234
vw	2470	vvw	5424
vvw	2646		

paramagnetic Ag(II) species from one another, thus providing for only weak coupling between them. The susceptibility closely obeys the Curie–Weiss law, as shown in Figure 3, and the small value of the Weiss constant ($\theta = -4.2$ (5)°) indicates that the material is magnetically dilute. This is consistent with Ag^{2+} separated by $[AgF_4]^-$ ions as in the formulation $Ag^{2+}[AgF_4]^-{}_2$. Bougon et al.[1,2] reported that their data for "AgF_3" obeyed the Curie–Weiss law over the temperature range 4–290 K. When the magnetic moment given by Bougon et al. for their "AgF_3" is adjusted to the formula Ag_3F_8, it becomes $\mu = 1.95 \pm 0.08\ \mu_B$, which is not significantly different from the effective magnetic moment found here: $\mu_{eff} = 1.924$ (3) μ_B. The equivalence of the magnetic and X-ray powder data for Ag_3F_8 to that reported by Bougon et al.[1,2] for their "AgF_3" proves the identity of the latter with the former.

The easy formation of $Ag^{II}Ag^{III}{}_2F_8$ and its much greater stability relative to AgF_3 indicate that the Ag(III) in this mixed-valence compound is less electronegative than in AgF_3. This is probably because, in $Ag^{II}Ag^{III}{}_2F_8$, the Ag(III) resides in a $[AgF_4]^-$ species. The salt formulation $Ag^{2+}[AgF_4]^-{}_2$ fits the known fluoro base properties of AgF_2 and the fluoro acid character of AgF_3. There are numerous examples of AgF_2 acting as a pseudo-alkaline-earth fluoride, in its formation of salts, and these have been well documented by Müller.[18] This basicity of AgF_2 is associated with the antibonding σ effect of the d^9 electron configuration of Ag(II), with the half-filled d orbital appreciably weakening the Ag(II)–F bonding. On the other hand, in the low-spin d^8 configuration, the fully vacant $d_{x^2-y^2}$ orbital provides for strong Ag–F bonding in the square-coordinated (xy-plane) Ag(III) species. Indeed, as has been demonstrated in this work, AgF_3, in AHF, is close in acidity to PF_5.

Because AgF_2 had also been shown by Gantar et al.[19,20] to be a monofluoro base in forming the salt $[AgF]^+[AsF_6]^-$ and by Žemva et al.[17] in making the salt $[AgF]^+[BF_4]^-$, it appeared probable that the related salt $[AgF]^+[AgF_4]^-$ (a 1:1 complex of AgF_2 and AgF_3) could also be made. This last material has added interest because of the likelihood of the cation being a chain polymer, with linearly and symmetrically coordinated Ag(II), as in the structure of $[AgF]^+[AsF_6]^-$ reported by Gantar et al.[20] In the absence of definitive structural evidence for the salt formulation $[AgF]^+[AgF_4]^-$, however, the 1:1 complex of AgF_2 and AgF_3 is referred to as $Ag^{II}Ag^{III}F_5$.

The compound $Ag^{II}Ag^{III}F_5$ was made by titrating a blue solution of $AgFAsF_6$ in AHF with an equimolar solution of $KAgF_4$ to precipitate a maroon solid, the supernatent then being colorless. The yield of solid satisfied

$$AgF^+ + AgF_4^- \rightarrow Ag_2F_5 \qquad (8)$$

The X-ray powder data are given in Table V.

Interaction of the $Ag^{II}Ag^{III}F_5$ with an additional 1 mol of AgF_3, in AHF, quickly gave $Ag^{II}Ag^{III}{}_2F_8$

$$Ag_2F_5 + AgF_3 \rightarrow Ag_3F_8 \qquad (9)$$

the X-ray powder diffraction pattern of which (see Table IV) was identical with that of Ag_3F_8 derived from the decomposition of AgF_3 (eq 2) or that from the interaction of $AgFAsF_6$ and BF_3 with AgF_4^- (eq 5).

Conclusions

AgF_3 is thermodynamically unstable, diamagnetic, and isostructural with AuF_3. Its powerful oxidizing properties are in harmony with the tight binding of its valence-shell d-orbital electrons. Mixed-valence 1:1 and 1:2 compounds of AgF_2 and AgF_3 may be the salts $[AgF]^+[AgF_4]^-$ and $Ag^{2+}[AgF_4]^-{}_2$.

Experimental Section

Materials. F_2 and BF_3 were from Matheson Gas Products, East Rutherford, NJ 07073, and PF_5 and AsF_5 were prepared[21] as follows, each being subjected to IR spectroscopy to check for common impurities. PF_5 was prepared by the reaction of phosphorus pentoxide with elemental fluorine under pressure. The fluorination of P_4O_{10} with elemental fluorine was carried out stepwise. Final fluorination conditions: pressure of elemental fluorine, 300 atm; temperature 250 °C; time 3 h. The obtained product was pure PF_5 without POF_3. AsF_5 was prepared similarly by fluorination of As_2O_3. Final reaction conditions: pressure of elemental fluorine, 150 atm; temperature, 250 °C; time, 3 h. Anhydrous HF (Matheson) was held at ~20 °C over solid K_2NiF_6 (Ozark Mahoning) to remove water. XeF_5AgF_4 was made as previously described.[5] $KAgF_4$ was prepared by the method of Hoppe[3] using $AgNO_3$ and KNO_3 (Fisher Scientific, certified quality) and also from an equimolar mixture of KF and AgF_2 with KrF_2 in AHF at ~20 °C with the procedure described[5] for XeF_5AgF_4. AgF_2 was prepared as previously described[17] and was kept under ClF_5 at 250 °C for several days. AgF was prepared by dissolving Ag_2O (Aldrich, Milwaukee, WI 53201) in AHF and evaporating the AHF from the decanted solution under vacuum at ~20 °C to yield an orange solid that was again treated with AHF to ensure removal of H_2O. $AgFAsF_6$ was prepared by dissolving AgF_2 in AHF as described by Gantar et al.[19] Translucent fluorocarbon polymer tubing (FEP) was obtained from CHEMPLAST Inc., Wayne, NJ 07470. WHITEY valves (1KS4) were obtained from Oakland Valve & Fitting Co., Walnut Creek, CA 94596.

Apparatus and Technique. A metal vacuum line, fluorine-handling equipment and Teflon valves were used as described previously.[6,17] For the majority of the novel preparations two $^3/_8$- or $^3/_4$-in.-o.d. FEP tubes, each sealed at one end, were joined at right angles to a Teflon Swagelock T compression fitting, which was also joined to a Teflon valve, previously described.[17] This T assembly was joined to the gas handling and vacuum system via a 1-ft. length of 1/4-in.-o.d. FEP tubing to provide for the decantation of AHF solutions from one of the legs of the T into the other. All Teflon apparatus was dried at ~20 °C under vacuum (10^{-3} Torr) for several hours and then exposed to AHF that had itself been dried over K_2NiF_6, this AHF then being discarded. A Monel Acco Helicoid pressure gauge (0–1400 Torr ± 0.3%) in conjunction with a calibrated volume, of which the gauge was part, were used to measure out gases, both those used as reagents and F_2 liberated in reactions. All solid fluorides were manipulated in the dry Ar atmosphere of a Vacuum Atmospheres Corp. DRILAB.

X-ray powder samples were prepared as previously described[17] except for AgF_3, which required particular care in handling. Samples of AgF_3 reacted incandescently with metal surfaces when frictional heat from scratching or grinding of the AgF_3 occurred. To minimize reduction of the AgF_3, it was transferred directly from the FEP tube in which it was prepared, to the neck of the quartz X-ray capillary (previously dried under vacuum at 500 °C). The powder was vibrated down the capillary by drawing a light-weight file across it. The powder was finally tamped into a well-packed column with a quartz ram-rod drawn to fit the 0.5- or 0.3-mm capillaries used for the samples. For the neutron diffraction experiments, 2-mm-o.d. capillaries, joined to a $^1/_4$-in.-o.d. tube and connected to a Whitey valve, were similarly filled to a length of 35 mm, two with AgF_3 (~50 mg each) and one with AuF_3 (100 mg). Loaded capillaries were plugged with dry Kel-F grease, removed from the

---

(18) Müller, B. G. *Angew. Chem., Int. Ed. Engl.* **1987**, *26*, 1081.

(19) Frlec, B.; Gantar, D.; Holloway, J. H. *J. Fluorine Chem.* **1982**, *20*, 385.

(20) Gantar, D.; Frlec, B.; Russell, D. R.; Holloway, J. H. *Acta Crystallogr.* **1987**, *C43*, 618.

(21) Jesih, A.; Žemva, B. *Vestn. Slov. Kem. Drus.* **1986**, *33*, 25.

DRILAB, and sealed by drawing down in a small flame.

AuF_3 Preparation. AuF_3 was prepared as previously described.[7]

AgF_3 Preparation. (a) XeF_5AgF_4 and AsF_5. XeF_5AgF_4 (1599.7 mg, 3.90 mmol) was loaded into the tube that formed part of the cross of the Teflon T apparatus, AsF_5 (3.90 mmol) and AHF (~5 mL) was condensed on to it at −196 °C, and the mixture was slowly warmed and stirred vigorously by a small Teflon-coated magnetic stirrer, controlled externally. A bright-red precipitate formed below −40 °C. (It was essential to avoid using excess AsF_5 or to have local molar excess of AsF_5 over the AgF_4^- salt since this led to loss of fluorine and $AgFAsF_6$ formation, with subsequent contamination of the AgF_3 with Ag_3F_8.) The precipitate was allowed to settle, and the AHF solution (containing XeF_5AsF_6) was decanted into the other FEP tube at right angles to it. The AHF from that tube was then distilled back under vacuum onto the AgF_3 at −196 °C. The AgF_3 was washed for 5 min with this AHF at ~20 °C, and the AHF decanted once more into the other leg of the apparatus. This cycle, for washing the AgF_3 free of XeF_5AsF_6, was repeated six times. The AgF_3 was finally dried at ~20 °C under dynamic vacuum, and the AHF-free FEP T was then transferred to the DRILAB. Raman spectroscopy showed[22] that the major product in the decantate leg of the FEP T was XeF_5AsF_6. The X-ray powder patterns of the bright-red solid frequently showed a weak line at $d \approx 3.7$ Å characteristic of the strongest reflection of Ag_3F_8. The samples also usually exhibited a very weak paramagnetism in accord with the presence of some Ag_3F_8 (q.v.).

(b) XeF_5AgF_4 and PF_5. Addition of PF_5 gas to a pale yellow solution of XeF_5AgF_4 in AHF produced a bright red precipitate, but only with a large molar excess of the PF_5 (~2 mol of PF_5/AgF_4^-). Removal of PF_5 resulted in redissolution of the AgF_3 to re-form XeF_5AgF_4. By decanting the AHF solution of XeF_5PF_6 and washing with fresh AHF saturated with PF_5, it was possible to isolate a high yield of the red solid, which X-ray powder photography showed was AgF_3.

(c) $KAgF_4$ and BF_3. Substitution of BF_3 gas for AsF_5 in procedure (a) provided a simpler and cleaner route to AgF_3. At ~20 °C, even with many minutes of vigorous stirring, in contact with BF_3-saturated AHF, AgF_3 showed no sign of interaction with the BF_3. Therefore, it was not necessary to limit the quantity of BF_3 to that of equimolarity with the $KAgF_4$. The gas was admitted slowly, to promote crystallinity of the AgF_3, and the KBF_4 formed in the reaction was removed by washing via decantation of the AHF solution, as for removal of XeF_5AsF_6 in the previous preparation. X-ray photography established the formation of KBF_4 from comparison with a standard pattern. The well-washed bright-red solid (usually in better than 95% yield, there being some losses associated with the washing by decantation) gave an X-ray powder pattern that was entirely indexable on the basis of the hexagonal cell reported below. Samples of AgF_3 prepared with BF_3 and used in establishing its diamagnetism were washed quickly to minimize decomposition. They were therefore contaminated with KBF_4.

(d) Analysis of AgF_3. Because of the steady loss of F_2 from AgF_3 in AHF, under the conditions necessary to wash it free of salts such as $KAsF_6$, XeF_5PF_6, or KBF_4, the composition was arrived at from a combination of several experiments. The quantity of fluorine liberated in the decomposition in AHF, $3AgF_3 \rightarrow Ag_3F_8 + {}^1/_2F_2$, was measured directly (q.v.). The nature of the solid product, Ag_3F_8, was determined by analysis and by its synthesis by other routes (q.v.). The diamagnetism of the freshly precipitated material (with BF_3) and its close structural relationship with AuF_3 (q.v.) combined with these other observations to settle the composition as AgF_3.

Synchrotron X-ray Powder Diffraction Data Collection and Structure Analysis for AgF_3. A wavelength of 1.248 05 Å was employed as a compromise between the conflicting requirements of minimizing the sample absorption, maintaining reasonable pattern resolution, and operating at an energy where the X-ray source had a high output. The data collected showed Bragg peaks with fwhm's greater than 0.18°, which is considerably in excess of instrumental resolution. All the peaks in the pattern, with the exception of a single weak line, were indexed on a hexagonal unit cell, $a = 5.0753$ (3) Å, $c = 15.448$ (1) Å (see Table III), similar to that of AuF_3. The unindexed diffraction maximum at $d \approx 3.7$ Å is attributable to the strongest Bragg reflection of a small amount of Ag_3F_8 impurity, the AgF_3 sample having been prepared (q.v.) from AsF_5.

Neutron Powder Diffraction Data Collection and Structure Analyses for AgF_3 and AuF_3. Details of the data collection are given in Table VI. The high-intensity powder diffractometer (HIPD) was chosen because the extremely high incident neutron intensity afforded the possibility of using small samples of these very reactive fluorides. The success of this approach can be seen in the quality of the diffraction patterns (Figure 4). The data collected in this way showed peaks down to ~0.6-Å d-spacing, all of which are fitted quite closely by the Rietveld refinement procedure and afforded a precise structure determination of both AgF_3 and AuF_3.

Table VI. Details of the Neutron Diffraction Data Collection for AgF_3 and AuF_3

instrument employed	Manuel Lujan, Jr., Neutron Scattering Center, Los Alamos National Laboratory, high-intensity power diffractometer (HIPD)
sample	100 mg of AgF_3 contained in two 2.0-mm-diameter quartz capillaries, sample length ~35 mm; 100 mg of AuF_3 contained in a 2.0-mm-diameter quartz capillary, sample length ~35 mm
diffraction geometry	9.0-m initial flight path, 1.25-m secondary flight paths to four each ${}^1/_2 \times 12''$ 10 atm ^{3}He detectors at ±153° 2θ
data collection	0.6 Å $\leq d \leq$ 4.8 Å in ~3800 constant $\Delta t/t$ steps for 10.85 h at 71.2-μA beam current for AgF_3 and for 4.19 h at 70.19 μA for AuF_3; range included 275 reflections for AgF_3 and 298 reflections for AuF_3

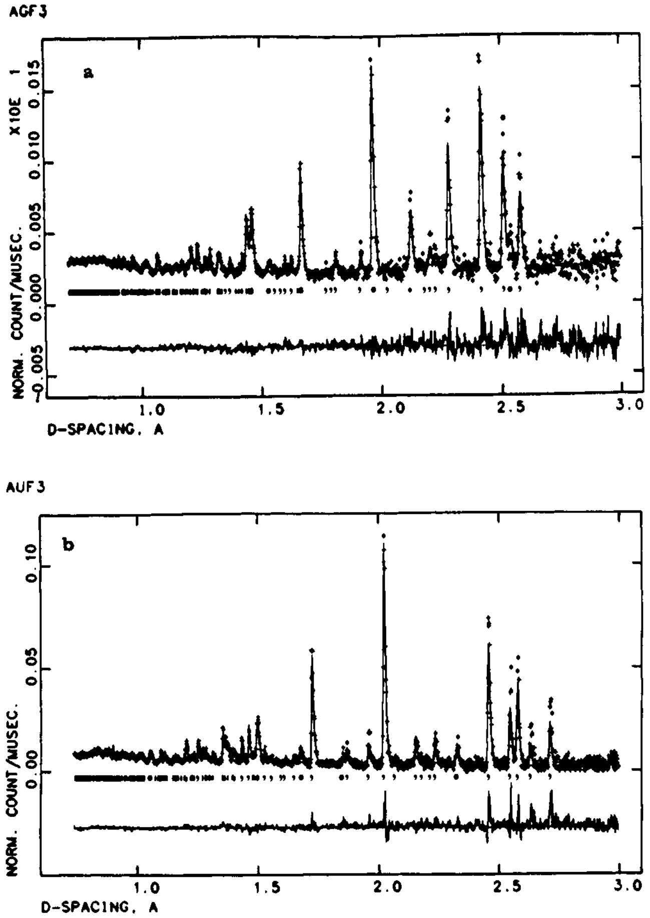

Figure 4. Portions of the fitted neutron time-of-flight powder diffraction patterns for data taken on the +153° 2θ bank on HIPD for (a) AgF_3 and (b) AuF_3. The observed values are shown as (+), and the calculated values from the best fit are shown as a curve. A difference ($I_{obs} - I_{calc}$) curve and the reflection positions are also shown. All intensity values are normalized by a previously measured incident spectrum.

Both structures were refined with the package GSAS[23] from neutron diffraction data collected at both ±153° 2θ for d spacings >0.6 Å. The results are given in Table VII. In both cases Fourier Series were used for the background and absorption coefficients were refined for each data set. For AgF_3 an extinction coefficient[24] was also refined; the value, 38 (8) μm^2, indicates that the average grain size was ~6 μm. No extinction effects were observed for AuF_3. The peak profiles were considerably

---

(22) Adams, C. J.; Bartlett, N. *Isr. J. Chem.* **1978**, *17*, 114.

(23) Larson, A. C.; Von Dreele, R. B. Los Alamos Laboratory Report No. LA-UR-86-748, 1987.

(24) Sabine, T. M.; Von Dreele, R. B.; Jorgensen, J.-E. *Acta Crystallogr.* **1988**, *A44*, 374.

Table VII. Final Models from Neutron Diffraction Structure Refinements for AgF_3 and AuF_3

	AgF_3[a]	AuF_3
space group	$P6_122$	$P6_122$
a/Å	5.0782 (2)	5.1508 (1)
c/Å	15.4523 (8)	16.2637 (7)
abs, +153°	−0.023 (5)	0.291 (14)
abs, −153°	−0.028 (5)	0.265 (13)
ext/μm^2	38 (8)	0
profile coeff		
$\sigma_1{}^2/\mu s/Å)^2$, +153°	77 (4)	50 (3)
$\sigma_1{}^2/\mu s/Å)^2$, −153°	119 (5)	91 (4)
$\sigma_{1a}{}^2/\mu s/Å)^2$, +153°	−17 (9)	−26 (5)
$\sigma_{1a}{}^2/\mu s/Å)^2$, −153°	−18 (12)	−45 (8)
A in 6(b): x, $2x$, $^1/_4$		
x	0.2694 (4)	0.2399 (3)
U_{iso}/Å^2	0.0112 (9)	0.0111 (8)
F(1) in 6(a): x, 0, 0		
x	0.2176 (8)	0.1639 (8)
U_{iso}/Å^2	0.0233 (12)	0.0215 (12)
F(2) in 12(c): x, y, z		
x	0.8401 (7)	0.7761 (6)
y	0.3186 (10)	0.3099 (7)
z	0.0054 (2)	0.0053 (2)
U_{iso}/Å^2	0.0350 (11)	0.0328 (10)
R_{wp}/%	6.21	11.21
R_p/%	3.83	7.58
χ^2	1.327	1.175

[a] The lattice constants for AgF_3 are slightly larger from the neutron experiment than from the synchrotron experiment. This difference is probably due to the slightly higher temperature in the neutron case and to the difficulty in estimating the exact scattering center in a time-of-flight experiment. As we are mainly interested in comparing AgF_3 and AuF_3, we have used the neutron data for calculating distances and angles.

broadened, and thus some of the coefficients of the peak shape function were also refined. Their values indicate that both materials exhibit a substantial degree of microstrain particularly perpendicular to the hexagonal axis.

Decomposition of AgF_3 in AHF. AgF_3 (985.9 mg, 5.98 mmol) prepared by precipitation from AgF_4^- with BF_3 was placed in an FEP tube connected through a Teflon valve to the Bourdon gauge. The volume of the closed system including the gauge was known. AHF (~6 mL at 20 °C) was transferred onto the AgF_3, and the mixture was stirred with a Teflon-coated stirrer bar. A noticeable darkening of the color of the AgF_3 occurred after 2 h, and this was accompanied by generation of gas that was not condensable at −196 °C. After 19 h, the suspended solid had become darker red-brown than AgF_3 and the gas evolution had ceased. The gas was IR inactive and reacted rapidly with clean Hg and was entirely consumed by it, this showing the gas to be F_2. The tensimetric measurements indicated 1.2 ± 0.3 mmol of F_2 liberated. X-ray powder photographs of the silver fluoride, remaining after removal of the F_2 and AHF, although indicative of poor crystallinity, showed it to be identical with the Ag_3F_8 prepared by the other routes (q.v.). In a separate experiment, 1.52 mmol of AgF_3 yielded 0.50 mmol of Ag_3F_8. Analysis of the solid product, from the 5.98-mmol AgF_3 sample, showed that it was slightly contaminated with KBF_4 (arising from the $KAgF_4$ interaction with BF_3). The BF_4^-, being kinetically stable in aqueous solution, did not contribute to the analysis for free F^-. Anal. Calcd for $Ag_3F_8{\cdot}0.13KBF_4$: Ag, 65.7; F, 30.8; B, 0.3; K 1.1. Found: Ag, 66.0; F, 31.2; B, 0.3; K. 1.1. The Ag to free F ratio is 3:8.05.

Interaction of AgF_3 with AsF_5 in AHF. AgF_3 (708.9 mg, 4.30 mmol) in AHF (~3 mL) was exposed to AsF_5 (4.30 mmol) at ~20 °C, and rapid dissolution of the AgF_3 occurred, to produce a deep blue solution, this being accompanied by the evolution of gas that was not condensable at −196 °C. This gas was shown to be F_2 by its quantitative interaction with clean Hg. Removal of AHF under vacuum yielded deep blue prismatic crystals, a single-crystal structural analysis of which, at −87 °C, proved (R_1 = 0.021, R_2 = 0.026) the material to be identical with $[AgF]^+[AsF_6]^-$ described by Gantar et al.[20] The yield of $AgFAsF_6$ was 1.53 ± 0.2 g (4.85 ± 0.63 mmol) (these large errors arising from uncertainty in the weight of the large FEP tube after exposure to AsF_5 in AHF). The yield of F_2 was 2.32 ± 0.4 mmol (theory 2.15 mmol). The findings were compatible with the reaction expressed in eq 4.

Oxidation of Xe by AgF_3. AgF_3 (483.1 mg, 2.93 mmol) in AHF (~5 mL) was exposed to a large molar excess of Xe gas at 20 °C. The bright red solid rapidly lost color and became dark brown. The mixture was allowed to interact at ~20 °C for 1 h, the tube was then cooled to −78 °C, and the excess Xe and AHF were removed under vacuum. After the mixture was warmed to ~20 °C, colorless crystals were observed on the walls of the tube, in addition to the dark brown solid in the bottom of it. This colorless material was transferred under vacuum to a trap. Raman spectroscopy showed a strong band at 496 cm^{-1}, characteristic[25] of XeF_2. The dark-brown silver fluoride remaining in the tube gave an X-ray powder photograph identical with that of authentic samples of face-centered orthorhombic[26] AgF_2. These observations are in accord with the reaction expressed in eq 6.

Oxidation of Xe by $KAgF_4$ in AHF. An orange solution of $KAgF_4$ (122.7 mg, 0.55 mmol) in AHF (5 mL) in an FEP tube was exposed to more Xe gas (2-atm of pressure at ~20 °C) than required to satisfy eq 7. The stirred mixture interacted rapidly to precipitate a dark brown solid, all color in the supernatant AHF solution having disappeared within 10 min. The AHF was removed under vacuum at −30 °C to leave a dark brown residue in the bottom of the tube and colorless crystals on the walls of it. The crystals were transferred, at 20 °C, under dynamic vacuum to a trap and were shown[25] by their strong Raman band at 496 cm^{-1} to be XeF_2. The involatile residue gave an X-ray powder photograph in which the AgF_2 pattern was prominent, the other lines probably arising from a mixture of KH_2F_3 and KH_3F_4. The total weight of solid product was 185.7 mg; that required for 0.55 mmol of AgF_2, 0.275 mmol of XeF_2, and 0.55 mmol of $KF{\cdot}2.5HF$ is 186.2 mg. The overall reaction is expressed by

$$2KAgF_4 + Xe + 2xHF \rightarrow 2AgF_2 + 2KF(HF)_x + XeF_2 \qquad 3 > x > 2$$

Preparation of $Ag^{II}Ag^{III}F_5$. $KAgF_4$ and $AgFAsF_6$ in AHF. $KAgF_4$ (238 mg, 1.07 mmol) dissolved in AHF (5 mL) contained in one leg of the FEP T apparatus was poured, at 20 °C, slowly into a solution of $AgFAsF_6$ (346 mg, 1.10 mmol) in AHF (~5 mL) in the leg at right angles to it. A maroon solid precipitated immediately. Some of the AHF was back-distilled into the $KAgF_4$ leg to wash any remaining $KAgF_4$ into the mixture. When the transfer of that salt was complete, the supernatant AHF solution was colorless. This colorless supernatant AHF was then decanted into the empty leg of the T and the AHF back vacuum distilled onto the maroon residue to wash that solid free of $KAsF_6$. The washing cycle was repeated 10 times, and the AHF was then removed under vacuum at 20 °C. An X-ray powder photograph of the maroon solid showed a sharp strong-line pattern of a new phase. Lines of $KAsF_6$, AgF_3, and AgF_2 were absent. The weight of the solid (326 mg) was appropriate for an almost quantitative yield of Ag_2F_5 (1.05 mmol).

Preparation of $Ag^{II}Ag^{III}{}_2F_8$. (a) $KAgF_4$ with $AgFAsF_6$ and BF_3. $KAgF_4$ (412 mg, 1.85 mmol) dissolved in AHF (~3 mL) in one leg of an FEP T apparatus was added slowly to a blue solution of $AgFAsF_6$ (313 mg, 0.99 mmol) dissolved in AHF (~5 mL). Immediate precipitation of a maroon solid (probably Ag_2F_5) occurred, the supernatant AHF solution retaining the orange coloration of dissolved AgF_4^-. To this mixture was then slowly added BF_3 with brisk stirring. The suspended solid rapidly became deep red-brown, as the AgF_4^- in the AHF was replaced by BF_4^-, and at the end point the supernatant AHF was colorless. This AHF solution (containing $KAsF_6$ and KBF_4) was decanted into the other leg of the FEP T, and the washing of the precipitate was carried out as in the preparation of Ag_2F_5. X-ray powder photography showed that the well-washed solid was free of $KAsF_6$ and KBF_4. There were no traces of Ag_2F_5, AgF_3, or AgF_2, and the pattern matched that of the product of the decomposition of AgF_3 in AHF. The yield of washed Ag_3F_8 was 397 mg (0.84 mmol, 90.5%).

(b) Ag_2F_5 and AgF_3 in AHF. A sample of Ag_2F_5 (176 mg, 0.57 mmol) was mixed with an equimolar quantity of AgF_3 (93 mg, 0.57 mmol) in an FEP tube, and AHF (6 mL) was vacuum distilled onto the mixture, which was then briskly stirred at ~20 °C. The color quickly changed to red-brown characteristic of Ag_3F_8, and the AHF was removed under dynamic vacuum after 1 h. X-ray powder photography (see Table IV) established that this material was identical with that formed in preparation (a) and in the decomposition of AgF_3 in AHF. No other silver fluorides were present. The stoichiometry of this preparation and that of preparation (a) confirmed that the composition must be Ag_3F_8.

Magnetic Susceptibility of Ag_3F_8. A sample of Ag_3F_8 (181 mg 0.380 mmol), prepared by route (a), was encapsulated in a Kel-F capsule previously passivated with F_2 and AsF_5. Magnetic susceptibility measurements, made at both 5 and 40 kG, over the temperature range 6–280 K, obeyed the Curie–Weiss law, with a Weiss constant θ = −4.2 (5)°, the susceptibility being field independent. The data are given in Figure 3. The effective magnetic moment μ_{eff} = 1.924 (3) μ_B.

---

(25) Smith, D. F. In *Noble Gas Compounds*; Hyman, H. H., Ed.; The University of Chicago Press: Chicago, London, 1963; p 295.

(26) Charpin, P.; Plurien, P.; Mereil, P. *Bull. Soc. Fr. Mineral. Cristallogr.* **1970**, *93*, 7.

Acknowledgment. The work carried out at Berkeley, Brookhaven, and Los Alamos was supported by the Director, Office of Energy Research, Office of Basic Energy Sciences, that at Berkeley by the Chemical Science Divison of the U.S. Department of Energy under Contract No. DE-AC03-67SF00098, that at Brookhaven by the Division of Materials Sciences, U.S. Department of Energy, under Contract DE-AC02-76CH0016, and that at Los Alamos under Contract No. W-7405-ENG-36. Additional support was provided by the U.S.-Yugoslav Joint Fund for Scientific and Technological Cooperation, in association with the National Science Foundation under Grant No. JF947. That part of the work carried out at the Institute Jožef Stefan was supported by the Secretariat for Research and Technology of Slovenia. We thank Professor K. S. Pitzer for valuable discussions concerning relativistic effects and Dr. G. V. Shalimoff for assistance with susceptibility measurements on Ag_3F_8. H.B. also gratefully acknowledges the Alexander von Humboldt Foundation for a Feodor Lynen Fellowship.

Macrocyclic Metal Complexes Built on Polyethylenimine

Junghun Suh,* Younghee Cho, and Kyung Joo Lee

Contribution from the Department of Chemistry, Seoul National University, Seoul 151-742, Korea.

Received November 8, 1990

Abstract: Metal centers with macrocyclic ligands are created on polyethylenimine (PEI) by the condensation of dicarbonyl compounds with PEI in the presence of transition-metal ions. The macrocycle-containing PEIs possess fixed multivalent cationic centers and exhibit much greater affinity for benzoate anions compared with the unmodified PEI. Complex formation with anionic ester 2-nitro-4-carboxyphenyl acetate was reflected in the saturation kinetic behavior observed for the deacylation of the ester promoted by the macrocycle-containing PEIs. On the basis of the kinetic data, it is proposed that the anionic substrate is anchored by the metal center upon complexation with the macrocycle-containing PEI derivative and that the amine nitrogen atom located close to the metal center attacks the acyl carbon on the bound ester.

Polyethylenimine (PEI) and its derivatives have been used as synzymes (*syn*thetic en*zymes*),[1] since complex formation with substrates and catalytic turnovers of the bound substrates are achieved.[1-5] PEI is obtained by polymerization of ethylenimine and, thus, contain the ethylamine moiety as the repeating unit. About 25% of the nitrogen atoms of PEI are primary amines, 50% are secondary amines, and 25% are tertiary amines. The tertiary nitrogen atoms are the branching points on the polymer skeleton. Polycationic microenvironment is provided by the positive charges located on the nitrogen atoms of the polymer backbone, and hydrophobic microenvironment is obtained on the polymer domain by attaching alkyl chains to the nitrogen atoms. Some polar organic functional groups introduced to the polymer by alkylation or acylation of the nitrogens behave as catalytic groups.

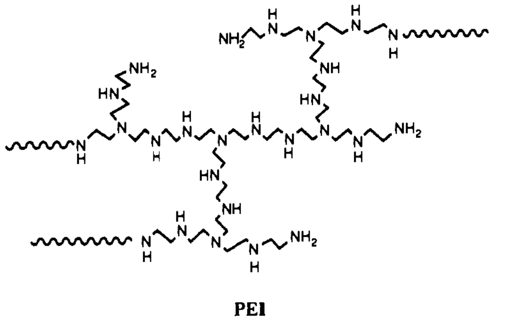

PEI

Catalytic activity of macrocyclic metal complexes[6] has been intensively investigated. Aldehyde hydration,[7,8] ester hydrolysis,[9] phosphate hydrolysis,[10] and molecular recognition of small organic molecules[11] are among the reactions in which macrocyclic metal complexes mimic metalloenzymes. Recently, the utility of macrocyclic complexes became more versatile by combining macrocyclic complexes with cyclodextrin derivatives[12] or antibodies.[13] Redox reactions such as olefin epoxidation[14] and oxygen reduction[15] also have been subject to catalysis by macrocyclic complexes.

Many of the multiaza macrocyclic metal complexes are prepared by the condensation of carbonyl compounds with polyamines in the presence of metal ions,[6] as exemplified by eq 1.[16] In this regard, PEI can be used as a synthon of the macrocyclic complex as well as the backbone of polymeric macrocycles. Since the ethylamine moiety is the repeating unit of PEI, it would be possible to prepare multiaza cyclic complexes with PEI. A typical commercial PEI has an average molecular weight of 60000, containing 1400 ethylamine moieties. Thus, a large number of macrocyclic

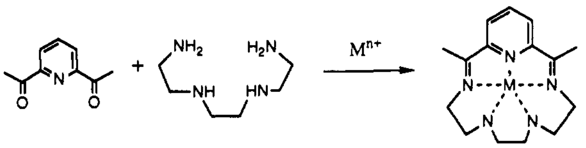

(1)

---

(1) Klotz, I. M.; Royer, G. P.; Scarpa, I. S. *Proc. Natl. Acad. Sci. U.S.A.* **1971**, *68*, 263.

(2) Suh, J.; Scarpa, I. S.; Klotz, I. M. *J. Am. Chem. Soc.* **1976**, *98*, 7060.

(3) Spetnagel, W. J.; Klotz, I. M. *J. Am. Chem. Soc.* **1976**, *98*, 8199.

(4) Delaney, E. J.; Wood, L. W.; Klotz, I. M. *J. Am. Chem. Soc.* **1982**, *104*, 799.

(5) Suh, J.; Klotz, I. M. *J. Am. Chem. Soc.* **1983**, *105*, 2373.

(6) (a) Mashiko, T.; Dolphin, D. In *Comprehensive Coordination Chemistry*; Wilkinson, G., Ed.; Pergamon: Oxford, 1987; Vol. 2, Chapter 21.1. (b) Curtis, N. F. In *Comprehensive Coordination Chemistry*; Wilkinson, G., Ed.; Pergamon: Oxford, 1987; Vol. 2, Chapter 21.2. (c) Mertes, K. B.; Lehn, J.-M. In *Comprehensive Coordination Chemistry*; Wilkinson, G., Eds.; Pergamon: Oxford, 1987; Vol. 2, Chapter 21.3.

(7) Woolley, P. *Nature* **1975**, *258*, 677.

(8) Kimura, E.; Shiota, T.; Koike, T.; Shiro, M.; Kodama, M. *J. Am. Chem. Soc.* **1990**, *112*, 5805.

(9) Chin, J.; Zou, X. *J. Am. Chem. Soc.* **1984**, *106*, 3687.

(10) Breslow, R.; Peter, R.; Gellman, S. H. *J. Am. Chem. Soc.* **1986**, *108*, 2388.

(11) Fujita, M.; Yazaki, J.; Ogura, K. *J. Am. Chem. Soc.* **1990**, *112*, 5645.

(12) Kuroda, Y.; Hiroshige, T.; Sera, K.; Shiroiwa, Y.; Tanaka, H.; Ogoshi, H. *J. Am. Chem. Soc.* **1989**, *111*, 1912.

(13) Cox, J. P. L.; Jankowski, K. J.; Kataky, R.; Parker, D.; Beeley, N. R. A.; Boyce, B. A.; Eaton, M. A. W.; Millar, K.; Millican, A. T.; Harrison, A.; Walker, C. *J. Chem. Soc., Chem. Commun.* **1989**, 797.

(14) Kinneary, J. F.; Albert, J. S.; Burrows, C. J. *J. Am. Chem. Soc.* **1988**, *110*, 6124.

(15) Collman, J. P.; Denisevich, P.; Konai, Y.; Marrocco, M.; Koval, C.; Anson, F. C. *J. Am. Chem. Soc.* **1980**, *102*, 6027.

(16) Nelson, S. M.; Busch, D. H. *Inorg. Chem.* **1969**, *9*, 1859.

0002-7863/91/1513-4198$02.50/0